Springer

KSME

Journal of Mechanical Science and Technology 25 (2) (2011) 333~339
www.springerlink.com/content/1738-494x
DOI 10.1007/s12206-010-1223-5

Magnetic field effect on fluid flow characteristics in a pipe for laminar flow †

Asadolah Malekzadeh[1,*], Amir Heydarinasab[1] and Bahram Dabir[2]

[1]*Chemical Engineering Department, Science and Research Branch, Azad University, Tehran, Iran*
[2]*Chemical Engineering Department, Amirkabir University of Technology, Tehran, Iran*

(Manuscript Received January 19, 2010; Revised October 22, 2010; Accepted November 22, 2010)

Abstract

The influence of a magnetic field on the skin friction factor of steady fully-developed laminar flow through a pipe was studied experimentally. A mathematical model was introduced and a finite difference scheme used to solve the governing equations in terms of vorticity-stream function. The model predictions agree favourably with experimental results. It is observed that the pressure drop varies in proportion to the square of the product of the magnetic field and the sine of the magnetic field angle. Also, the pressure drop is proportional to the flow rate. This situation is similar to what applies in the absence of a magnetic field. It is found that a transverse magnetic field changes the axial velocity profile from the parabolic to a relatively flat shape. At first, the radial velocity rises more rapidly and then gradually decreases along the pipe until falling to zero. A numerical correlation can be written for the considerable distance required for the new axial velocity profile to establish. Owing to the changes taking place in the axial velocity profile, it exhibits a higher skin friction factor. The new axial velocity profile asymptotically approaches its limit as the Hartmann number becomes large.

Keywords: Fluid flow characteristics; Laminar flow; MHD flow; Magnetic field

1. Introduction

There has been considerable interest in studying flow characteristics of electrically-conducting fluids because of its many practical applications such as in electronic components, chemical processing equipment, high-temperature plasmas, cooling of nuclear reactors, liquid metal fluids, MHD accelerators, and power generation systems. In the long history of the study of an electrically-conducting fluid flow, a great deal of effort has been made to understand the interaction between a magnetic field and fluid flow characteristics. The effect of a transverse magnetic field on the structure of a turbulent flow was examined by Gardner and Lykoudis [1, 2]. They reported that the turbulence intensity decreased to a laminar level over a broad range of Reynolds numbers and magnetic fields. The effect of Magnetic field on steady laminar flow of a Newtonian fluid over a vertical flat plate was studied numerically by Rashad [3]. The flat plate embedded in a porous media in the presence of thermophoresis particle deposition effect. Furthermore, the steady laminar boundary-layer flow past a wedge immersed in an incompressible micropolar fluid was investigated theoretically by Ishak et al. [4]. A variable magnetic field applied normal to the walls of the wedge. They observed a reduction in the velocity boundary-layer thickness as the strength of wall-normal magnetic field became large. Damseh et al. [5] considered the problem over a horizontal plate and reported that increasing the magnetic influence number increases the skin friction factor. Abd-el-Malek and Helal [6] solved the problem of an unsteady laminar flow under the effect of a magnetic field normal to the plate. Referring to the numerical results, they observed that the velocity boundary-layer thickness becomes smaller for the increase in the magnetic influence number. Sivasankaran and Ho [7] investigated numerically the effect of magnetic field on flow in a rectangular enclosure. Recently, Abdelkhalek [8] investigated this problem using a perturbation technique and reported that the imposed magnetic field diminishes the wall shear. The properties of human blood as well as blood vessels and the magnetic field effect were the subjects of interest for several researchers [9-12]. Very recently, Tashtoush and Magableh [13] considered numerically the influence of a magnetic field on the fluid flow characteristics of blood flow in multi-stenosis arteries and reported an increase in the skin friction factor. The present work aims to investigate the problem in a pipe. Here, a complete analysis of flow through a pipe is discussed in the entry region and the fully-developed region. Pipe flow is considered due to its practical applications. Full Navier-Stokes equations in cylindrical coordinates are introduced and solved using the vorticity stream function approach. Obviously, the inclusion of the magnetic field angle as an inde-

† This paper was recommended for publication in revised form by Editor Haecheon Choi

*Corresponding author. Tel.: +989121957234, Fax: +982614302182
E-mail address: asad.malekzadeh@gmail.com

pendent variable in the governing partial differential equations increases the complexity of the problem. This problem is considered in the present study. There has been no experimental study that confirms the correctness of the numerical results. Thus, a series of experiments is carried out to determine the influence of a magnetic field in a pipe for laminar flow.

2. Experimental apparatus

Fig. 1(a) shows a schematic view of the present experimental system. A potassium hydroxide (KOH) 30 wt% water solution is used in this experiment because of low electrical conductivity of pure water. The KOH water solution flow is introduced into the horizontal pipe test section by mechanical pump.

Fig. 1(b) shows the details of the test section. The test section of this loop is made of a 3.5 m long copper pipe with an inner diameter of 19, 23, or 35 mm. A series of constant magnetic fields is applied for 1.5 m along the pipe. Two pressure probes having a diameter of 10 mm are fixed at two holes of uniform diameter along the length of the pipe. The location of probes is shown in Fig. 1(b). The effect of magnetic field on the probes is negligible because the sheathed probes used in this test section are insulated. However, the measured pressure difference was stable when the magnetic field was constant. There is a pressure measuring scanner connected to the pressure probes whose outputs are recorded in a personal computer.

Table 1. The properties of 30 wt% KOH water solution.

		T=35 (°C)
Density	ρ (kg/m^3)	1279
Dynamic viscosity	μ (kg/ms)	0.00152
Electrical conductivity	σ (1/Ω*m)	75.2

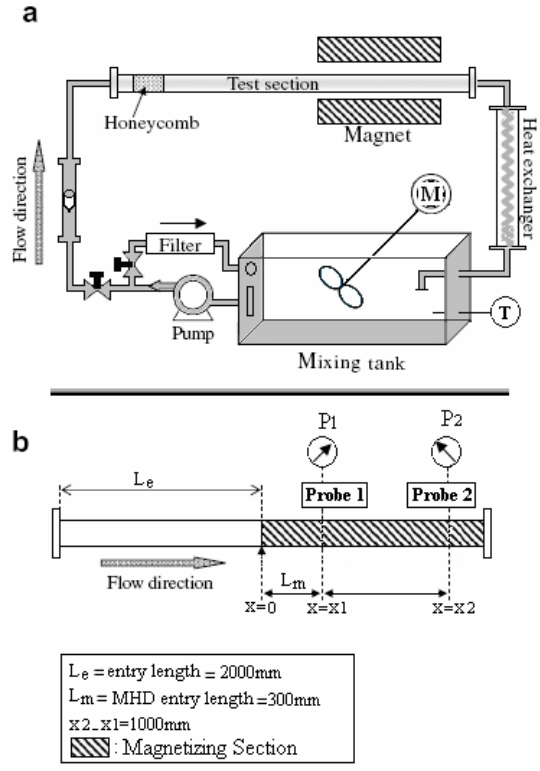

Fig. 1. Experimental set-up: (a) Overall view and (b) Details of test section.

The KOH water solution properties at 35(°C) are mentioned in Table 1. The KOH water solution flow rate is measured by means of a rotameter. The rotameter is calibrated with the KOH water solution by means of weighting for a given period of time. The Reynolds number based on bulk velocity and pipe diameter is set to 1000, 1500, and 2000 for seven Hartmann numbers; Ha = 0, 2.5, 5, 7.5, 10, 12.5, and 15. The bulk velocity is calculated by the flow rate and the cross section of the pipe.

As can be expected in the entrance of the Magnetizing section an entry length L_m is required in which the effect of magnetic field is stabled. More detailed discussion about the influence of all governing parameters on this new entry length will be presented later.

3. Mathematical model

If we apply a magnetic field on an electrically conducting fluid, an electromagnetic force will be produced due to the interaction of current with the magnetic field. The electromotive force generated by a magnetic field is known to be proportional to the speed of motion and the magnetic flux intensity **B**. The current density **J** is defined as:

$$\mathrm{J} = \sigma(\mathrm{E} + \mathrm{V} \times \mathrm{B}) \tag{1}$$

where σ denotes the electrical conductivity, **E** is the electrical field intensity and **V** is the velocity vector. The electromagnetic force $\mathbf{F_m}$ to be included in the momentum equation is:

$$\mathrm{F_m} = \mathrm{J} \times \mathrm{B} = \sigma(\mathrm{V} \times \mathrm{B}) \times \mathrm{B}\,. \tag{2}$$

It is also assumed that the uniform magnetic field $\mathbf{B} = B_x\mathbf{e_x} + B_r\mathbf{e_r}$ of constant magnitude $B = (B_x^2 + B_r^2)^{1/2}$ is applied, where $\mathbf{e_x}$ and $\mathbf{e_r}$ are unit vectors in cylindrical coordinates. The orientation of the magnetic field forms an angle ϕ with the horizontal axis (the flow direction) such that $\tan\phi = B_r / B_x$.

The following assumptions are taken for this study. The density and viscosity of the fluid are constant. The Flow is two-dimensional, laminar and incompressible. Under the above assumptions the continuity and Navier-Stokes equations may be written as follows:

$$\frac{\partial v}{\partial r} + \frac{v}{r} + \frac{\partial u}{\partial x} = 0 \tag{3}$$

$$u\frac{\partial u}{\partial x}+v\frac{\partial u}{\partial r}=-\frac{1}{\rho}\frac{\partial p}{\partial x}+\frac{\mu}{\rho}(\frac{\partial^2 u}{\partial r^2}+\frac{1}{r}\frac{\partial u}{\partial r}+\frac{\partial^2 u}{\partial x^2}) + \frac{\sigma B^2}{\rho}(v\sin\phi\cos\phi-u\sin^2\phi) \tag{4}$$

$$u\frac{\partial v}{\partial x}+v\frac{\partial v}{\partial r}=-\frac{1}{\rho}\frac{\partial p}{\partial r}+\frac{\mu}{\rho}(\frac{\partial^2 v}{\partial r^2}+\frac{1}{r}\frac{\partial v}{\partial r}-\frac{v}{r^2}+\frac{\partial^2 v}{\partial x^2}) + \frac{\sigma B^2}{\rho}(u\sin\phi\cos\phi-v\cos^2\phi) \tag{5}$$

where u and v are the velocity components in the x and r directions, respectively. The following non-dimensional parameters are used:

$$X=\frac{x}{R},\quad \hat{r}=\frac{r}{R},\quad U=\frac{u}{u_0},\quad V=\frac{v}{u_0},\quad P=\frac{p}{\rho u_0^2}$$

After nondimensionalization, the governing equations can be rewritten as:

$$\frac{\partial V}{\partial \hat{r}}+\frac{V}{\hat{r}}+\frac{\partial U}{\partial X}=0 \tag{6}$$

$$U\frac{\partial U}{\partial X}+V\frac{\partial U}{\partial \hat{r}}=-\frac{\partial P}{\partial X}+\frac{2}{\mathrm{Re}}(\frac{\partial^2 U}{\partial \hat{r}^2}+\frac{1}{\hat{r}}\frac{\partial U}{\partial \hat{r}}+\frac{\partial^2 U}{\partial X^2}) + \frac{2Ha^2}{\mathrm{Re}}(V\sin\phi\cos\phi-U\sin^2\phi) \tag{7}$$

$$U\frac{\partial V}{\partial X}+V\frac{\partial V}{\partial \hat{r}}=-\frac{\partial P}{\partial \hat{r}}+\frac{2}{\mathrm{Re}}(\frac{\partial^2 V}{\partial \hat{r}^2}+\frac{1}{\hat{r}}\frac{\partial V}{\partial \hat{r}}-\frac{V}{\hat{r}^2}+\frac{\partial^2 V}{\partial X^2}) + \frac{2Ha^2}{\mathrm{Re}}(U\sin\phi\cos\phi-V\cos^2\phi) \tag{8}$$

where $Ha = BR\,(\sigma/\mu)^{1/2}$ denotes the Hartmann number and $Re=\rho u_0 D/\mu$, is the Reynolds number.

From Eqs. (7) and (8), the vorticity equation takes the form:

$$V\frac{\partial \omega}{\partial \hat{r}}+U\frac{\partial \omega}{\partial X}-V\frac{\omega}{\hat{r}}=\frac{2}{\mathrm{Re}}(\frac{\partial^2 \omega}{\partial X^2}+\frac{1}{\hat{r}}\frac{\partial \omega}{\partial \hat{r}}+\frac{\partial^2 \omega}{\partial \hat{r}^2}-\frac{\omega}{\hat{r}^2}) + \frac{2Ha^2}{\mathrm{Re}}\left[\sin\phi\cos\phi(\frac{\partial U}{\partial X}-\frac{\partial V}{\partial \hat{r}})+(\sin^2\phi\frac{\partial U}{\partial \hat{r}}-\cos^2\phi\frac{\partial V}{\partial X})\right]. \tag{9}$$

The equation for stream function is as follows:

$$E^2\psi=\frac{\partial^2 \psi}{\partial X^2}-\frac{1}{\hat{r}}\frac{\partial \psi}{\partial \hat{r}}+\frac{\partial^2 \psi}{\partial \hat{r}^2}=-\omega\hat{r}\,. \tag{10}$$

The corresponding boundary conditions can be written as:

$$X=0:\quad \psi=\hat{r}^2-\frac{\hat{r}^4}{2},\quad U=2(1-\hat{r}^2),\quad V=0,\quad \omega=4\hat{r}$$

$$X\to\infty:\quad \frac{\partial^2 \psi}{\partial X^2}=0,\quad \frac{\partial U}{\partial X}=0,\quad \frac{\partial V}{\partial X}=0,\quad \omega=-\frac{\partial}{\partial \hat{r}}(\frac{1}{\hat{r}}\frac{\partial \psi}{\partial \hat{r}})$$

$$\hat{r}=0:\quad \psi=0,\quad \frac{\partial U}{\partial \hat{r}}=0,\quad V=0,\quad \omega=0$$

$$\hat{r}=1:\quad \frac{\partial \psi}{\partial X}=0,\quad U=0,\quad V=0,\quad \omega=-\frac{\partial^2 \psi}{\partial \hat{r}^2}.$$

The velocity components using the stream function are calculated from the following:

$$U=\frac{1}{\hat{r}}\frac{\partial \psi}{\partial \hat{r}},\quad V=-\frac{1}{\hat{r}}\frac{\partial \psi}{\partial X}\,. \tag{11}$$

Eqs. (9)-(11) represent a system of coupled and non-linear partial differential equations which are solved numerically under the boundary conditions using the finite difference approximations. Finite difference equations relating the variables are obtained by writing the equations at the mid point of the computational cell and then replacing the different terms by their second order central difference approximations. It is observed from the grid independence test that a 100 × 4000 uniformly spaced grid is enough to investigate the problem. Smaller step sizes do not show any significant changes in the results. The resulting algebraic equation for vorticity is solved using iterative method whereas Successive Over Relaxation (SOR) method is used to solve the equation for the stream function. Relaxation is designed to enhance convergence. Thus, having calculated the vorticity values at iteration k+1, using their respective solutions given at k (k = 0 corresponds to the initial guesses), the stream function is solved at this advanced step. The resulting stream function values are then used to determine the velocity components and the boundary values of the vorticity. Then, the sequence beginning with the solution of the vorticity equation is applied and repeated until the desired accuracy of results is obtained. Five-decimal accuracy is employed as the criterion for convergence.

Once the flow field of the fluid is calculated, the skin friction factor C_f is obtained from the following relation:

$$C_f=-\frac{\mu(\partial u/\partial r)_{r=R}}{0.5\rho u_0^2}=\frac{4}{\mathrm{Re}}(-\frac{\partial U}{\partial \hat{r}})_{\hat{r}=1}. \tag{12}$$

4. Results and discussion

Fig. 2 shows the variation of the skin friction factor against the magnetic field influence for steady MHD fully-developed laminar flow of an electrically conducting fluid through a pipe. In the experimental work, a series of constant magnetic fields in parallel and perpendicular to the flow direction was applied and no significant effect on the pressure drop was observed when the flow direction and the direction of magnetic field were parallel to each other. The following equation shows how to calculate the skin friction factor using experimental data when the direction of magnetic field is perpendicular to the flow direction.

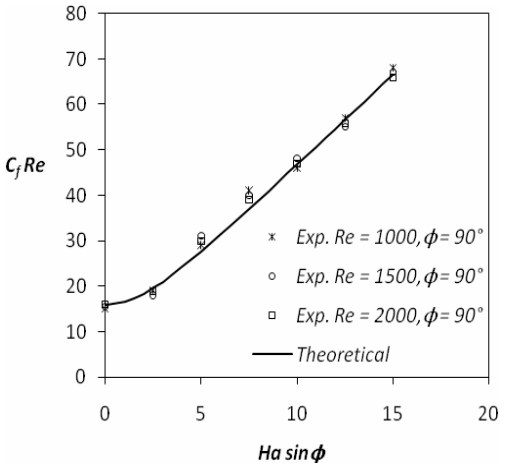

Fig. 2. Skin friction factor against magnetic field influence for MHD fully-developed laminar pipe flow.

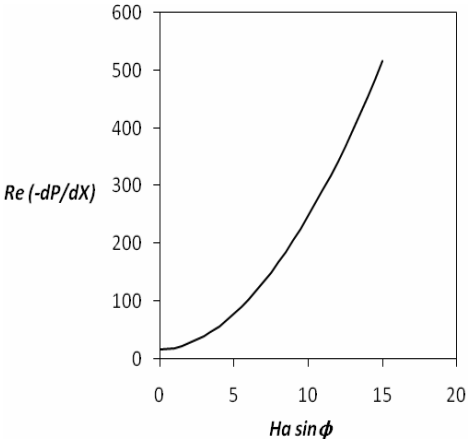

Fig. 3. Dimensionless pressure gradient against Magnetic field influence for MHD fully-developed laminar pipe flow.

$$C_f = (\frac{R}{L})(\frac{p_1 - p_2}{\rho u_0^2}) - \frac{\sigma B^2 R}{\rho u_0} \quad (13)$$

where $p_1 - p_2$ is the pressure difference between $x = x_1$ and $x = x_2$ as shown in Fig. 1(b).The model predictions agree favourably with experimental results. As shown in Fig. 2, the influence of magnetic field can be diminished by reducing the angle between the flow direction and the direction of magnetic field.

It is found that C_f is inversely proportional to Re^1 because $C_f Re$ is independent of *Re*. this situation is similar to what happens in the absence of a magnetic field. It is observed that the skin friction factor rises almost linearly with the magnetic field. Thus, the skin friction factor increases with an increase in the magnetic field which in turn increases the pressure drop and pumping power.

Fig. 3 shows the dimensionless pressure gradient through the pipe for steady MHD fully-developed laminar flow. Because *Re (-dP/dX)* is independent of *Re,* the pressure drop is

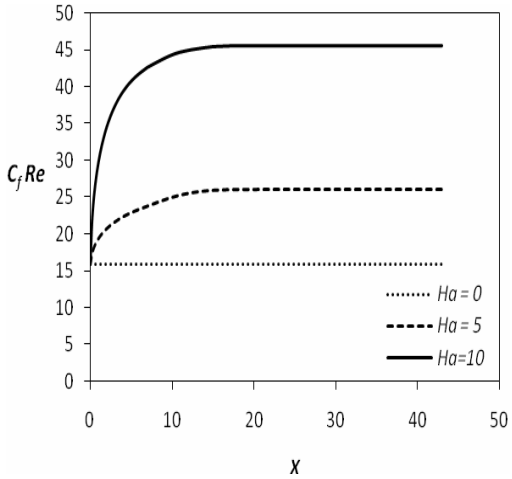

Fig. 4. skin friction factor along pipe for different values of Ha at *Re* = 1000 and $\phi = 90°$.

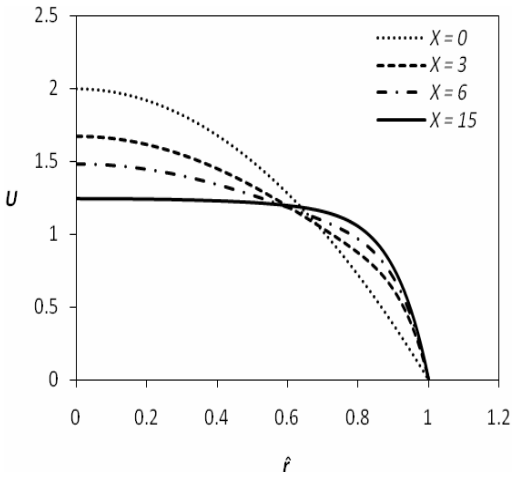

Fig. 5. Dimensionless axial velocity profile for different values of X at *Re* = 1000, *Ha* = 10, and $\phi = 90°$.

proportional to the flow rate. This situation is similar to what applies in the absence of a magnetic field. It is also observed that the pressure drop varies in proportion to the square of the product of the magnetic field and the sine of the magnetic field angle.

Fig. 4 shows the difference in skin friction factor between *Ha* = 0 and *Ha* = 5, 10 at *Re* = 1000 and $\phi = 90°$. The horizontal axis is the dimensionless distance from the starting point of applying the magnetic field. It is logical to suppose that the magnetic force acts as a resistive drag force. This force is directly proportional to the velocity. In both laminar and turbulent flow the velocity is zero at the wall and has a maximum value at the centre-line and hence the resistive drag force is zero at the pipe wall and increases to a maximum at the centre. This non-uniform force distribution reduces the axial flow velocity of the central stream of the pipe. The axial flow velocity near the pipe wall will increase because the fluid flows to the region close to the pipe wall in order to keep uniform mass flow. Thus, an increase in the velocity gradient

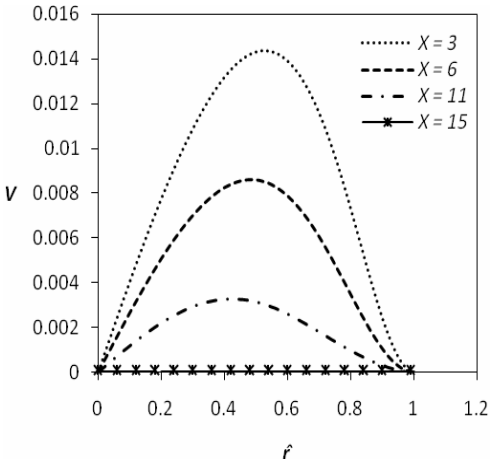

Fig. 6. Dimensionless radial velocity profile for different values of X at Re = 1000, Ha = 10, and ϕ = 90°.

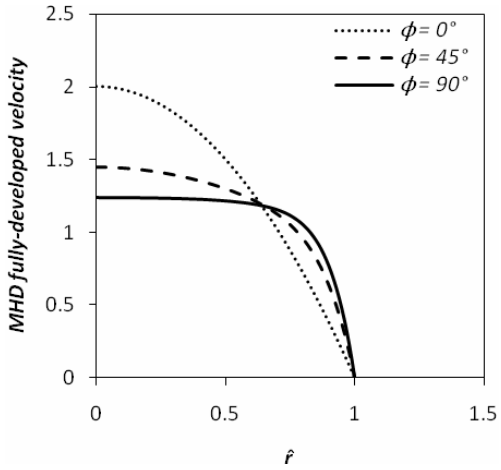

Fig. 8. Dimensionless MHD fully-developed velocity profile for different values of ϕ at Re = 1000 and Ha = 10.

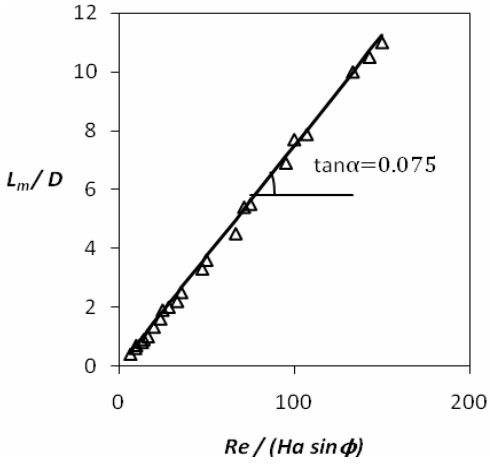

Fig. 7. Dimensionless MHD entry length for the velocity profile to adjust from the fully-developed to the MHD fully-developed pattern.

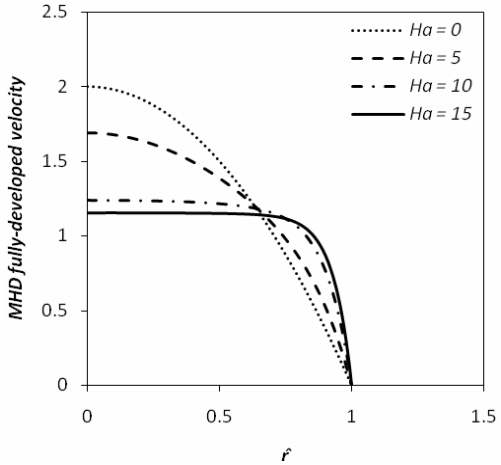

Fig. 9. Dimensionless MHD fully-developed velocity profile for different values of Ha at Re = 1000 and ϕ = 90°.

occurs at the pipe wall which in turn raises the shear stress at the pipe wall and hence produces an increase in the skin friction factor. The axial flow velocity of the central stream of the pipe gradually reduces in the direction of flow and the skin friction factor increases until a new fully-developed velocity profile is established. Once established, the velocity profile remains constant and so the skin friction factor reaches its maximum.

Fig. 5 shows that the magnetic field changes the axial velocity profile from the parabolic to a relatively flat shape. The flow is fully-developed at the starting point of applying the magnetic field (X = 0). As the dimensionless distance becomes larger, the velocity profile changes until the new fully-developed velocity profile is obtained (X = 15). The new velocity profile, namely the MHD fully-developed velocity profile, is much flatter over most of the diameter and remains unchanged until the fluid reaches the region where the magnetic field ends. For this profile, the velocity of the fluid is zero at the pipe wall but rises as the distance from the pipe wall increases and eventually approaches the velocity of the bulk of the stream.

Fig. 6 shows the dimensionless radial velocity profile which is zero at the pipe wall but rises as the distance from the pipe wall increases and finally approaches zero again at the centreline. At first, the radial velocity rises more rapidly and then gradually decreases along the pipe until falling to zero (X = 15). Beyond this point, the flow will be again one-dimensional and the MHD fully-developed velocity profile will dominate.

It is to be noted that in case the magnetic field is removed, the velocity profile starts to change until the MHD fully-developed profile is replaced by the fully-developed profile.

However, a considerable distance is required for the velocity profile to adjust from the fully-developed to the MHD fully-developed pattern when a constant magnetic field is applied. The region where the velocity profile is gradually adjusted is called as MHD entry length. For fully-developed laminar flow of an electrically conducting fluid through a pipe, the MHD entry length L_m can be obtained numerically over a wide range of Reynolds numbers at different values of magnetic fields when the direction of magnetic field is perpendicu-

lar or parallel to the flow direction or at some angle in between.

The results are summarized in a plot of L_m/D against $Re/(Ha \sin\phi)$ on ordinary Cartesian coordinates as shown in Fig. 7. The plot is a straight line of slope 0.075 and therefore an approximate numerical expression for the MHD entry length is found as:

$$\frac{L_m}{D} = 0.075 \frac{\mathrm{Re}}{Ha \sin\phi}. \tag{14}$$

Fig. 8 shows the difference in dimensionless MHD fully-developed velocity profile between $\phi = 0°$ and $\phi = 45°$, $90°$ at Re =1000 and Ha = 10. When $\phi = 90°$, the velocity profile is flatter than the other two angles of the magnetic field. It is also shown that when $\phi = 0°$, the velocity profile is parabolic. This situation is identical to what occurs in the absence of a magnetic field. A similar result was found in the experimental work for the pressure drop and the friction factor. Thus, a magnetic field has no effect on fluid flow characteristics while the direction of magnetic field is parallel to the flow direction.

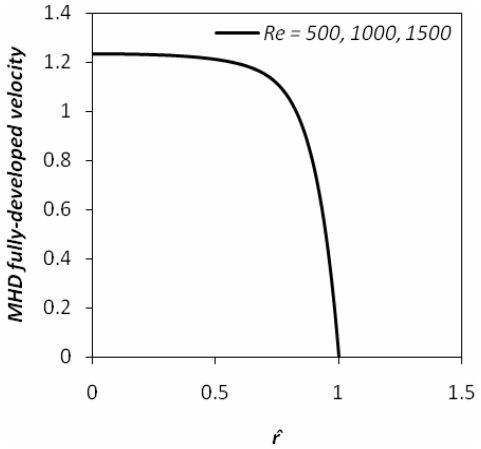

Fig. 10. Dimensionless MHD fully-developed velocity profile for different values of Re at Ha = 10 and $\phi = 90°$.

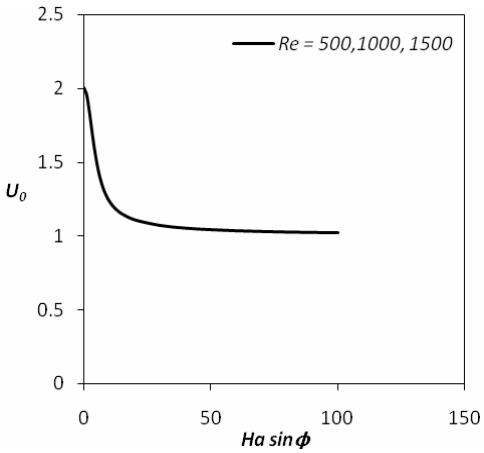

Fig. 11. Dimensionless centre-line axial velocity against magnetic field influence for different values of Re.

The different in dimensionless MHD fully-developed velocity profile at Re = 1000 and $\phi = 90°$ is shown in Fig. 9 as the value of magnetic field is changed. The MHD fully-developed velocity profile becomes flatter with an increase in the value of Hartmann number which in turn increases the velocity gradient at the pipe wall and hence produces an increase in the skin friction factor.

The value of Reynolds number has no effect on the dimensionless MHD fully-developed velocity profile as shown in Fig. 10. This is valid both in the presence and in the absence of a magnetic field because $Re\ (-dP/dX)$ is independent of Re both in the presence and in the absence of a magnetic field. Although the plots corresponding to Re = 500 and Re = 1000, 1500 are all identical to each other in Fig. 10, their MHD entry lengths are significantly different because the MHD entry length is proportional to the Reynolds number and inversely proportional to the product of the Hartmann number and the sine of the magnetic field angle (Eq. 14).

Fig. 11 shows that further increase of the magnetic field influence has no considerable effect on the centre-line axial velocity when the Hartmann number exceeds a certain value. Beyond the value $(Ha \sin\phi) \simeq 10$, all MHD fully-developed velocity profiles are very close to each other. In fact, the MHD fully-developed velocity profile asymptotically approaches its limit as the Hartmann number becomes larger.

5. Conclusions

In the experimental work, it is observed that the skin friction factor rises almost linearly with the magnetic field when a steady fully-developed laminar flow is subjected to a series of transverse magnetic fields. The present numerical results are in good agreement with the experimental work. The present model is able to predict the flow characteristics of an electrically conducting fluid through a pipe in the presence of a magnetic field. It is shown that the pressure drop varies in proportion to the square of the product of the magnetic field and the sine of the magnetic field angle. Also, the pressure drop is proportional to the flow rate. This situation is similar to what applies in the absence of a magnetic field. No significant effect on fluid flow characteristics is observed when the flow direction and the direction of magnetic field are parallel to each other. The velocity profile starts to change until the fully–developed profile is replaced by a MHD fully-developed profile as a transverse magnetic field is applied. The MHD fully-developed profile is much flatter over most of the diameter and remains unchanged until the fluid reaches the region where the magnetic field ends. At first, the radial velocity rises more rapidly and then gradually decreases along the pipe until falling to zero. A new entry length is required for the velocity profile to adjust from the fully-developed to the MHD fully-developed pattern. A correlation formula is given for the new entry length as a function of Hartmann number, sin of the magnetic field angle, Reynolds number, and the pipe diameter. It is also found that the value of Reynolds number has no ef-

fect on the dimensionless MHD fully-developed velocity profile. The MHD fully-developed velocity profile becomes flatter with an increase in the value of Hartmann number and asymptotically approaches its limit.

Acknowledgment

The authors wish to acknowledge sincere gratitude to each of reviewers for valuable comments. They express their thanks to Mr. M. Hashemi for his technical assistance in the experiment and to Mrs. L. Shahabi, former graduate student, for her valuable assistance in the measurements.

Nomenclature

$\mathbf{B}$	:	Magnetic field intensity, T
C_f	:	Skin friction factor
D	:	Pipe diameter, m
$\mathbf{E}$	:	Electric field intensity, V/m
$\mathbf{F_m}$	:	Electromagnetic force, kg/m^2s^2
Ha	:	Hartmann number
$\mathbf{J}$	:	Current density, Amp/m^2
L	:	Length of the pipe between $x = x_1$ and $x = x_2$ as shown in Fig. 1b, m
L_m	:	MHD entry Length, m
p	:	Pressure, pa
R	:	Pipe radius, m
Re	:	Reynolds number
u	:	Axial velocity, m/s
U	:	Dimensionless axial velocity
u_0	:	Average velocity at inlet, m/s
v	:	Radial component of velocity, m/s
V	:	Dimensionless radial velocity
$\mathbf{V}$	:	Velocity vector. , m/s
x	:	Axial coordinate, m
r	:	Radial coordinate, m
X, $\hat{r}$	:	Dimensionless coordinates
ϕ	:	Direction of the magnetic field
μ	:	Dynamic viscosity, kg/ms
ρ	:	Density, kg/m^3
σ	:	Electrical conductivity, 1/Ωm
ω	:	Vorticity
ψ	:	Stream function

References

[1] R. A. Gardner and P. S. Lykoudis, Magneto-fluid-mechanic pipe flow in a transverse magnetic field part 1. Isothermal flow, *J. Fluid Mech.,* 47 (1) (1971) 737-764.

[2] R. A. Gardner and P. S. Lykoudis, Magneto-fluid-mechanic pipe flow in a transverse magnetic field part 2. Heat transfer, *J. Fluid Mech.,* 48 (1) (1971) 129-141.

[3] A. M. Rashad, Influence of radiation on MHD free convection from a vertical flat plate embedded in porous media with thermophoretic deposition of particles, *Commun. Nonlinear Sci. Numer. Simul.,* 13 (2008) 2213-2222.

[4] A. Ishak, R. Nazar and I. Pop, MHD boundary-layer flow of a micropolar fluid past a wedge with constant wall heat flux, *Commun. Nonlinear Sci. Numer. Simul.,* 14 (2009) 109-118.

[5] R. A. Damseh, H. M. Duwairi and M. Al-Odat, Similarity analysis of magnetic field and thermal radiation effects on forced convection flow, *Turkish J. Eng. Env. Sci.,* 30 (2006) 83-89.

[6] M. B. Abd-el-Malek and M. M. Helal, Similarity solutions for magneto-forced-unsteady free convective laminar boundary-layer flow, *J. Comput. Appl. Math.,* 218 (2008) 202-214.

[7] S. Sivasankaran and C. J. Ho, Effect of temperature dependent properties on MHD convection of water near its density maximum in a square cavity, *Int. J. Therm. Sci.,* 47 (2008) 1184-1194.

[8] M. M. Abdelkhalek, Heat and mass transfer in MHD flow by perturbation technique, *Comp. Mater. Sci.,* 43 (2008) 384-391.

[9] E. E. Shehawey, E. Elbarbary, N. Afifi and M. Elshahed, MHD flow of an elastic-viscous fluid under periodic body acceleration, *Int. J. Mech. Sci.,* 23 (2000) 795-799.

[10] V. Kirkovskaya and Y. Mukharskaya, Influence of a variable magnetic field on the rheological properties of blood in treatment of rheumatoid arthritis, *Int. J. Thermophys,* 76 (2003) 708-714.

[11] K. Perktold and G. Rappitsch, Computer simulation of local blood flow and vessel mechanics in a compliant carotid artery bifurcation model, *J. Biomech.,* 28 (1995) 845-856.

[12] K. Rai and S. Rai, Heat transfer inside the tissues with a supplying vessel for the case when metabolic heat generation and blood perfusion are temperature dependent, *Heat Mass Transfer,* 35 (1999) 345-350.

[13] B. Tashtoush and A. Magableh, Magnetic field effect on heat transfer and fluid flow characteristics of blood flow in multi-stenosis arteries, *Heat Mass Transfer,* 44 (2008) 297-304.

Asadolah Malekzadeh was a research staff at the NIOC from 1997 until 2005. He received the Ph.D. degree in chemical engineering from IAU in 2009 and joined the department of chemical engineering, IAUG in 2010.